Supporting information:

Structural Comparison of Mouse and Human α-Synuclein Amyloid Fibrils by Solid-State NMR

Guohua Lv[1], Ashutosh Kumar[1], Karin Giller[1], Maria L. Orcellet[2], Dietmar Riedel[3], Claudio O. Fernández[2], Stefan Becker[1], and Adam Lange[1]*

[1] Department of NMR-Based Structural Biology, Max Planck Institute for Biophysical Chemistry, Am Fassberg 11, 37077 Goettingen, Germany

[2] Instituto de Biología Molecular y Celular de Rosario, Consejo Nacional de Investigaciones Científicas y Técnicas, Universidad Nacional de Rosario, Suipacha 531, S2002LRK Rosario, Argentina

[3] Laboratory for Electron Microscopy, Max Planck Institute for Biophysical Chemistry, Am Fassberg 11, 37077 Goettingen, Germany

*Corresponding author: Phone: +49 551 201-2214, fax: +49 551 201-2202, email: adla@nmr.mpibpc.mpg.de.

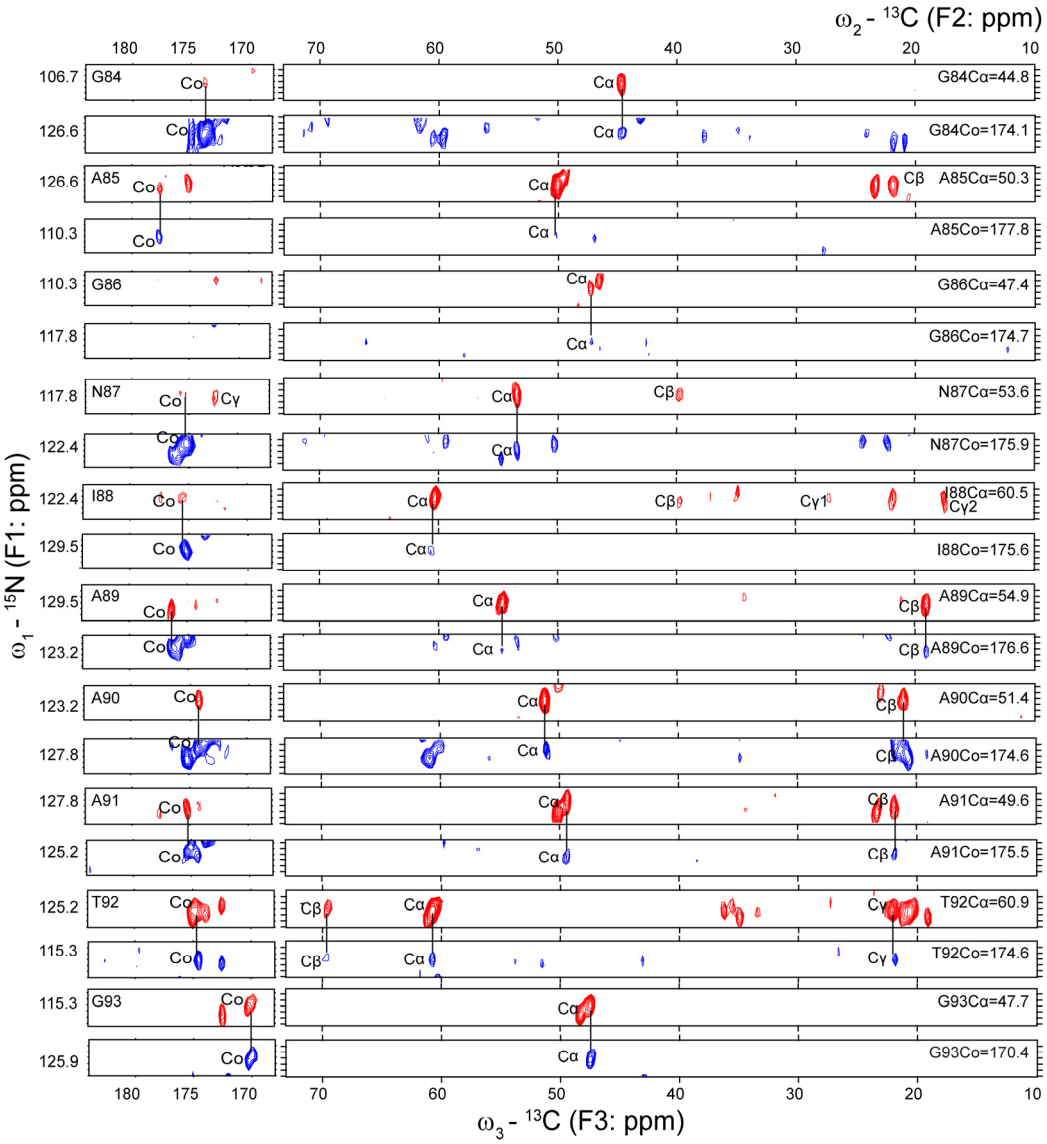

Figure S1. Strip plots from 3D NCACX (red) and 3D NCOCX (blue) spectra of [U-^{13}C/^{15}N]-labeled mAS fibrils, showing the sequential resonance assignment of Gly84-Gly93. Both spectra were recorded at 20 T and 11 kHz magic-angle spinning.

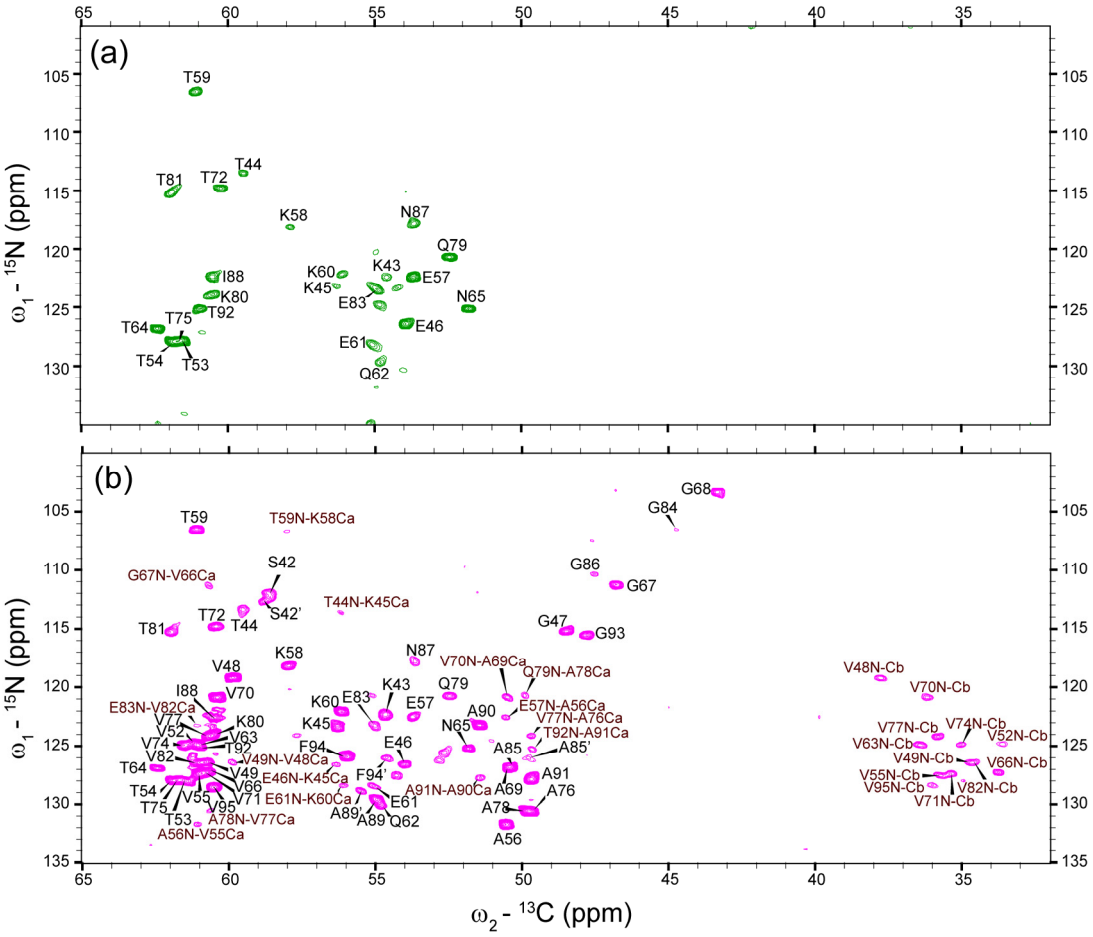

Figure S2. $^{15}N/^{13}C$ correlation spectra of sparsely ^{13}C labeled mAS fibrils. NCA spectra of (a) [1-^{13}C]Glc-labled mAS fibrils and (b) [2-^{13}C]Glc-labeled mAS fibrils. $^{15}N(i)$-$^{13}C\alpha(i)$ correlations are indicated in black, while $^{15}N(i)$-$^{13}C\alpha(i-1)$ correlations and $^{15}N(i)$-$^{13}C\beta(i)$ correlations of Val are indicated in dark red. Both spectra were recorded at 20 T and 11 kHz magic-angle spinning.

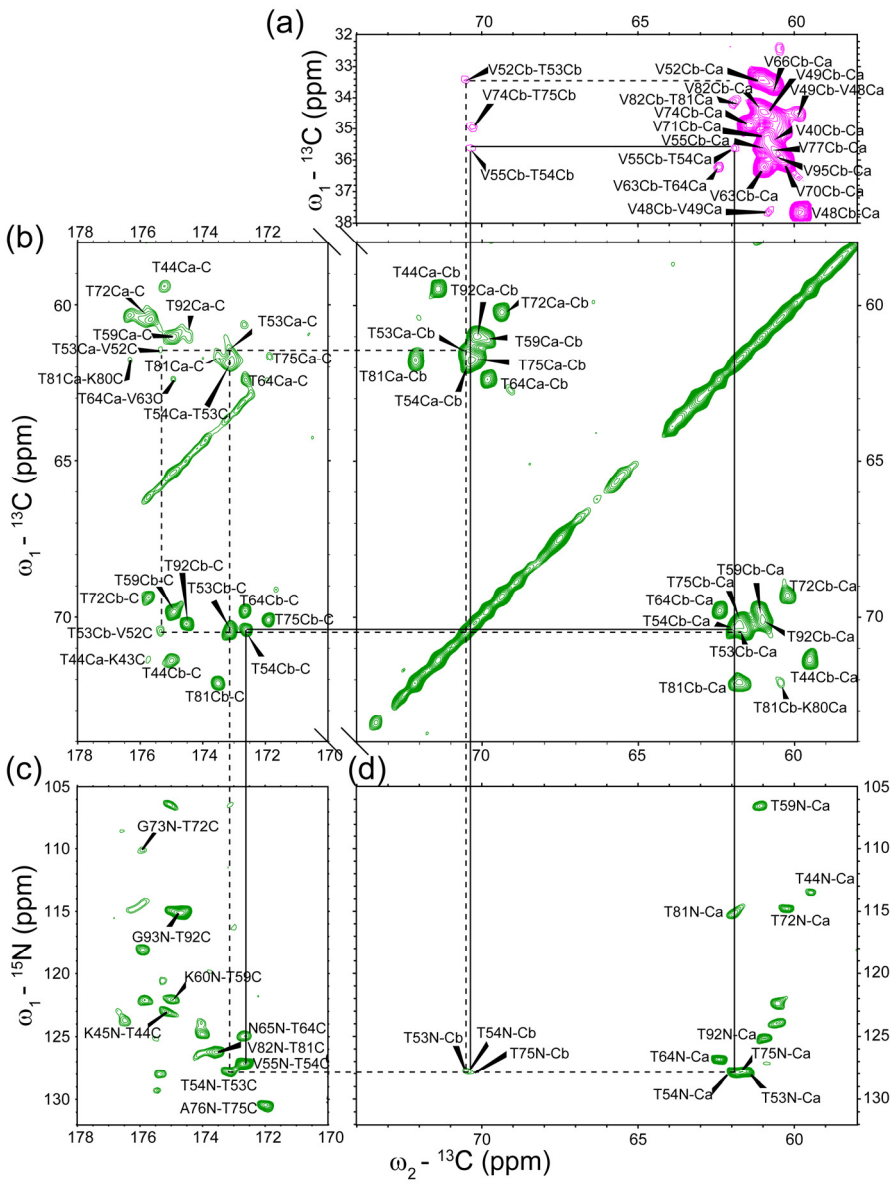

Figure S3. Sequential resonance assignment of Thr and Val residues using [1-^{13}C]Glc- (in green, b-d) and [2-^{13}C]Glc-labeled mAS fibrils (in magenta, a). (a) Excerpt of the Val Cβ region of a 2D PDSD spectrum recorded with a mixing time of 700 ms, (b) 2D PDSD spectrum with a mixing time of 400 ms, (c) NCO, and (d) NCA spectra. The assignment of the 9 Thr residues in the rigid core of mAS fibrils is illustrated. Broken and continuous lines correspond to the assignment of Thr53 and Thr54, respectively. Spectra shown in (a, b) and (c, d) were recorded at 18.8 T and 20 T, respectively, and at 11 kHz magic-angle spinning.

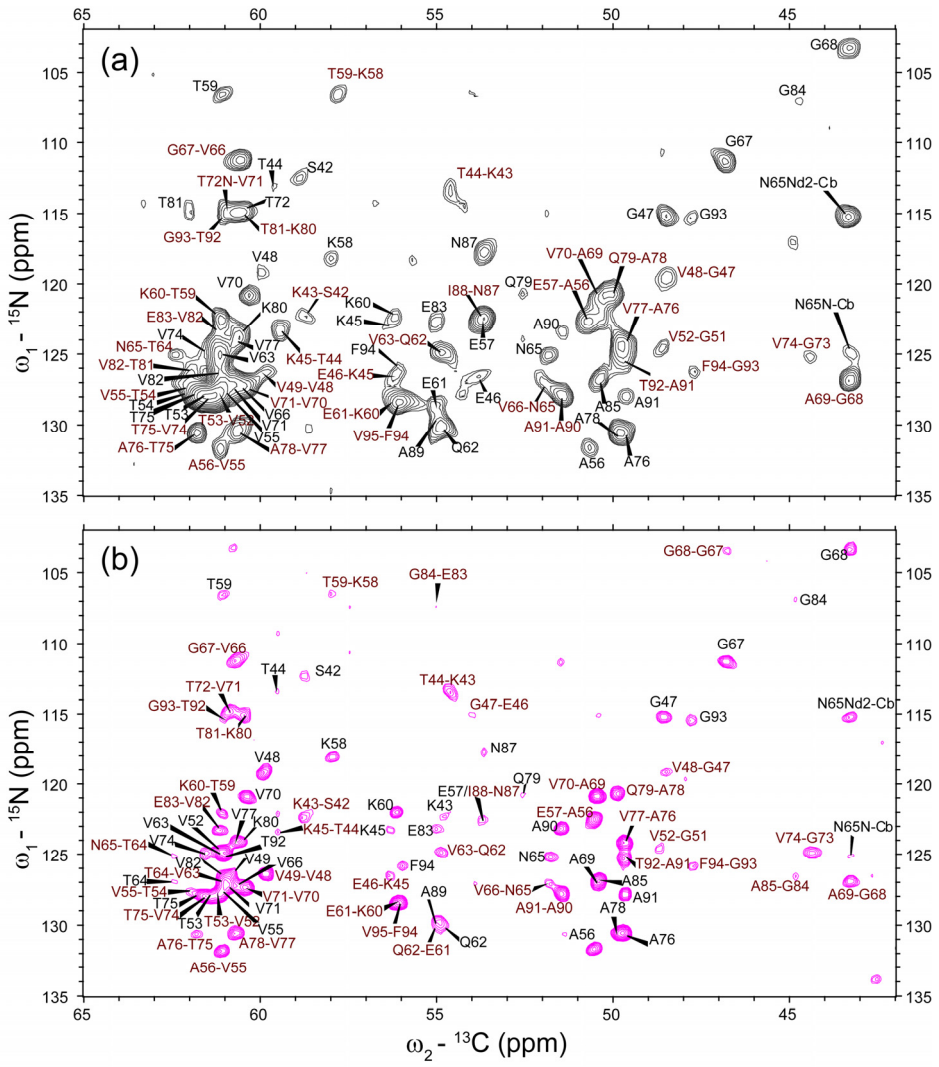

Figure S4. Secondary structure analysis using NHHC spectra recorded on (a) [U-^{13}C/^{15}N]-labeled mAS fibrils and (b) [2-^{13}C]-Glc-labeled mAS fibrils. The ^{15}N(i)-^{13}Cα(i) and ^{15}N(i)-^{13}Cα(i-1) correlations are labeled in black and dark red, respectively. Both spectra were recorded at 20 T and 11 kHz magic-angle spinning.

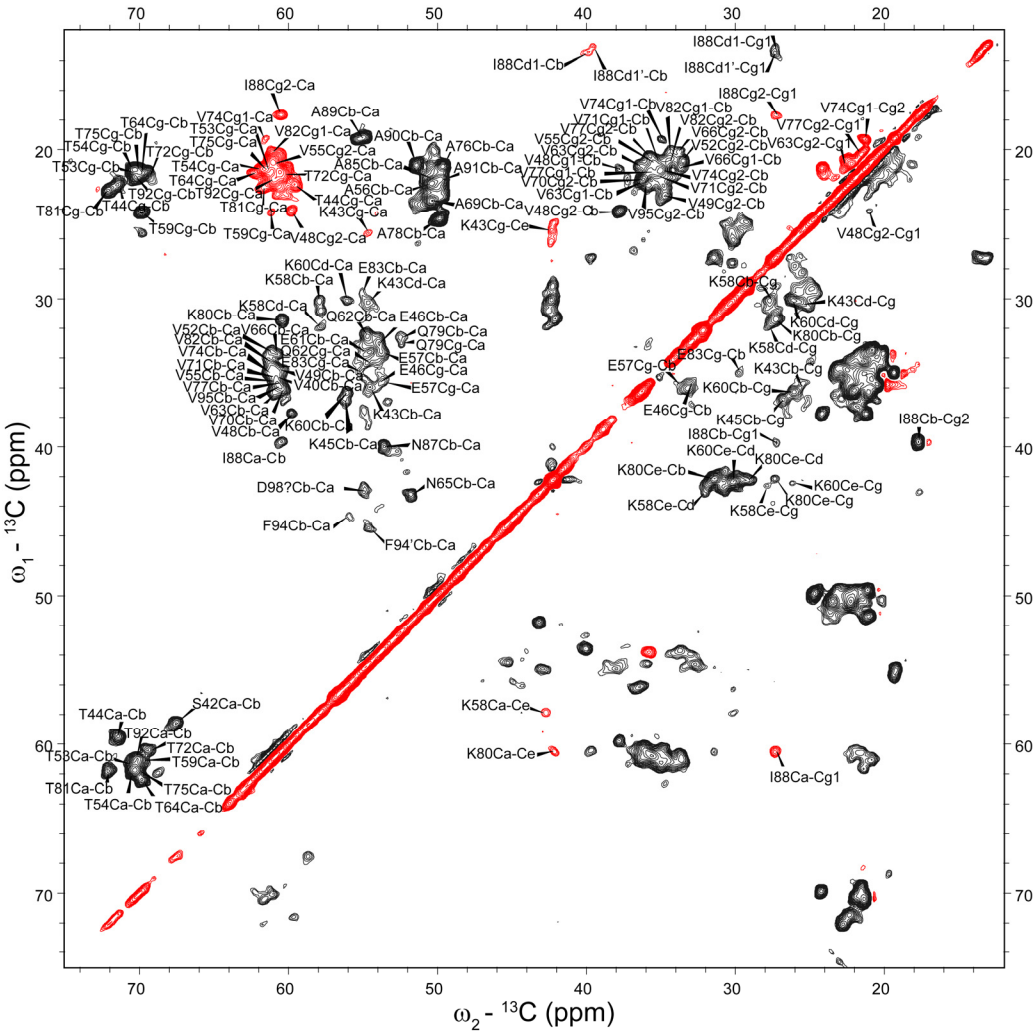

Figure S5. DREAM spectrum of [U-^{13}C/^{15}N]-labeled mAS fibrils. The spectrum was recorded at 18.8 T and 18 kHz magic-angle spinning. Note, only one Ser resonance is visible in the spectrum (corresponding to Ser42). Positive contours are shown in red and negative contours in black.

Table S1. Chemical shift assignments for mAS fibrils.

Res.	N	C′	Cα	Cβ	Cγ2/1	Cδ	Cε	Cz	Nsc
Ser?	-	-	58.3	63.9					
Val40*	-	-	60.4	35.2	-/-				
Gly41	119	174.7	47.9						
Ser42	112.2	171.5	58.7	67.6					
Lys43	122.3	175.7	54.6	35.8	25.6	30.2	42.1		-
Thr44	113.4	175.2	59.5	71.4	22.4				
Lys45	123.3	173.5	56.2	36.8	26.8	-	42.2		-
Glu46	126.5	174.6	53.9	32.9	35.6	183.1			
Gly47	115.1	172.6	48.4						
Val48	119.2	174.1	59.8	37.7	24.2/21.2				
Val49	126.3	174.6	60.8	34.6	23.1/-				
His50	-	-	-	-	-	-	-		-/-
Gly51	-	174.9	48.6						
Val52	124.7	175.3	61.1	33.5	20.7/-				
Thr53	127.8	173.1	61.6	70.4	21.2				
Thr54	127.9	172.7	61.9	70.4	21.2				
Val55	127.5	174.2	61	35.7	21.2/-				
Ala56	131.6	175.3	50.5	22.3					
Glu57	122.5	175.9	53.7	33.6	35.7	183.3			
Lys58	118.1	175	57.9	30.1	27.6	31.9	42.5		34.1
Thr59	106.5	175	61.1	69.8	24.2				
Lys60	122.1	175.3	56.1	36.3	26.1	30.1	42.3		29.9
Glu61	128.4	174.3	55	33.7	-	-			
Gln62	130	174	54.7	32.5	34.2	179.9			111.9
Val63	124.9	175	61	36.3	21/22.2				
Thr64	126.9	172.7	62.4	69.8	21.5				
Asn65	125.1	172.7	51.7	43.2	175				115.2
Val66	127.2	178.5	60.7	33.7	19.9/21.1				
Gly67	111.2	172.8	46.7						
Gly68	103.4	172.2	43.3						
Ala69	126.9	175.3	50.4	23.4					
Val70	120.8	174.4	60.3	36.1	21.9/-				
Val71	127.3	176.5	60.8	35.3	21.7/20.7				
Thr72	114.7	175.9	60.3	69.4	21.7				
Gly73	110.6	173.7	44.3						
Val74	124.9	175.3	61.5	35	21.3/19.2				
Thr75	127.9	172	61.7	70.1	21.1				
Ala76	130.5	174.1	49.6	21.2					
Val77	124.1	172.7	60.6	35.8	20.3/21.5				
Ala78	130.5	176.2	49.8	24.7					
Gln79	120.6	176.4	52.4	32.6	32.9	177.7			111.2
Lys80	123.8	176.2	60.5	31.4	27.3	29.2	42.1		33.2
Thr81	115	173.6	61.8	72	22.7				
Val82	126.3	174.2	61.1	34.4	20.5/20.1				
Glu83	123.4	173	54.9	29.5	34.9	183.9			
Gly84 (**)	106.7	174.1 (173.2)	44.8 (44.6)						

Ala85	126.6	177.8	50.3	21.9					
(**)	(125.8)		(49.7)						
Gly86	110.3	174.7	47.4						
(**)			(47.3)						
Asn87	117.8	175.9	53.6	39.9	172.9				116.6
Ile88	122.4	175.6	60.5	39.7	17.7/27.3	13.4			
(**)						(13.1)			
Ala89	129.5	176.6	54.9	19.3					
(**)			(55.4)						
Ala90	123.2	174.6	51.4	21.2					
Ala91	127.8	175.5	49.6	21.9					
Thr92	125.2	174.6	60.9	70.2	21.8				
Gly93	115.3	170.4	47.7						
(**)			(47.5)						
Phe94	125.9	-	55.9	45.1	136.4	132.1	130.9	-	
(***)	(126)	(173.5)	(54.6)	(45.5)	(138.1)	(132.2)	(129.3)	(-)	
Val95	128.5	-	60.5	35.9	22.4/-				
Asp?	-	-	54.9	42.9	-				
Pro?	-	-	62.9	32.1	27.3	50.7			

(*) The assignment of Val40 is ambiguous.

(**) Resonances in brackets indicate peak doubling.

(***) Phe94 has a second set of resonances (Phe94').